

# Estimation of initial conditions for generating moving ILMs from wavenumber-frequency spectrum of static ILMs in FPU-NKG mixed lattice

Kosuke Kawasaki<sup>†</sup> and Masayuki Kimura<sup>‡</sup> and Shinji Doi<sup>‡</sup>




<sup>†</sup>Graduate School of Engineering, Kyoto University  
 Kyoto-Digaku Katsura, Saikyo-ku, Kyoto 615-8530, Japan

<sup>‡</sup>Faculty of Engineering, Setsunan University  
 17-8 Ikedanakamachi, Neyagawa, Osaka 572-0074, Japan  
 Email: kawasaki@rotary.kuee.kyoto-u.ac.jp

**Abstract**—Intrinsic localized mode (ILM) is localized vibration of energy in nonlinear coupled oscillator arrays. Estimating the initial conditions of moving ILMs are required to investigate the characteristics of moving ILMs. In this report, initial conditions of moving ILMs are generated from the frequency-wavenumber spectrum of static ILMs. The Fourier spectrum of static ILMs is tilted in the frequency-wavenumber domain. The slope depends on the velocity of moving ILMs. In addition, the spectrum of the static ILMs is expanded to the next Brillouin zones by using the Gaussian function. The estimated initial conditions successfully generate long-lived moving ILMs with desired velocities.

## 1. Introduction

Spatially localized vibration in nonlinear coupled oscillator arrays is called intrinsic localized mode (ILM) or discrete breather (DB). This phenomenon was first discovered by Seivers and Takeno in Fermi-Pasta-Uram (FPU) lattice[1]. Generally, ILM is caused by discreteness and nonlinearity of the system. Therefore, ILM is identified in various physical systems[2]. The ILM is also known can be moved for a long distance without the decay of its energy concentration. This implies that the moving ILM can be a carrier of kinetic energy. In Ref.[3], moving ILMs were experimentally studied on cyclic electric nonlinear transmission lines. Moving ILMs have also been numerically studied on two-dimensional hexagonal nonlinearity lattice[4]. For further studies on moving ILMs, a precise estimation of the initial conditions for generating moving ILMs is necessary. Various methods of initial value estimation have been studied and successfully generated relatively slow-moving ILMs[5]. However, the initial condition for fast-moving ILM generates not only the moving ILM but also the small amplitude waves. In this report, we discuss the estimation of initial conditions of moving ILMs using the spectrum of static ILMs in the wavenumber-frequency domain.

ORCID iDs Kosuke Kawasaki:  0000-0002-8306-918X, Masayuki Kimura:  0000-0002-1445-6266, Shinji Doi:  0000-0001-7046-8635

## 2. ILM in frequency-wavenumber domain

In this report, we consider a system as follows:

$$\frac{d^2 u_n}{dt^2} = -\alpha_1 u_n - \alpha_2 (2u_n - u_{n-1} - u_{n+1}) - \beta_1 u_n^3 - \beta_2 (u_n - u_{n-1})^3 - \beta_2 (u_n - u_{n+1})^3 \quad (1)$$

where  $n = 1, \dots, N$  and  $N$  denotes the total number of oscillators. This system is called mixed lattice because Eq.(1) becomes FPU lattice ( $\alpha_1 = 0, \beta_1 = 0$ ) and nonlinear Klein-Gordon lattice ( $\beta_2 = 0$ ). The boundary conditions are periodic in this study. The other parameters are set at  $\alpha_1 = 0, \alpha_2 = 1, \beta_1 = 0.625$  and  $\beta_2 = 0.375$ .

Let us consider a nonlinear map

$$F : \{u_n(t)\} \rightarrow \{u_{n+r}(t+T)\}. \quad (2)$$

This is a combination of the time evolution map and lattice unit translation map, thus, the map that translates the original solution by an integer lattice unit  $r$  after time  $T$  has passed. Moving ILMs corresponds to a fixed point of the map. Then the Newton-Raphson method is applied to compute the moving ILM. We call them “numerically exact moving ILM”. Note that we choose  $r = 1$  and the number of oscillations during  $T$  is half-integer like 1.5, 2.5, ..., 10.5. Static ILMs are also obtained as a fixed point of the map when  $r = 0$ . Let  $T_c$  and  $\omega_c$  be the vibration period and frequency of oscillators.

Figure 1 shows the Fourier spectrum of numerically exact static and moving ILMs in the wavenumber-frequency domain which is obtained by 2D-FFT of the spatio-temporal trajectories of each ILM. In Fig.1, the dispersion relation for the linearized Eq.(1) is also shown by white line. Since we consider the hard potential model as Eq.(1), spectral distribution is located above the dispersion relation. For static ILMs, the frequency is constant regardless of the wavenumber. On the other hand, for the moving ILM, the spectral distribution appears with a slope that is proportional to the velocity of moving ILMs. In Ref.[6], a two-dimensional Fourier transform of a moving Gaussian pulse in a continuous medium is given, and it is shown that the spectrum component in the wavenumber-frequency do-



This work is licensed under a Creative Commons Attribution NonCommercial, No Derivatives 4.0 License.

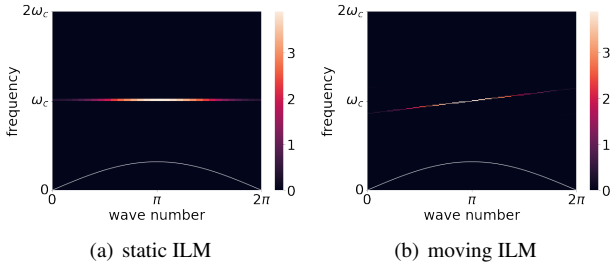


Figure 1: wavenumber-frequency domain

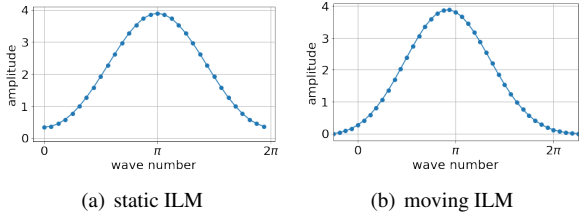


Figure 2: Distribution of the spectrum

main has a slope corresponding to the moving velocity, and the same result is obtained in the discrete system.

Figure 2 shows the wavenumber-frequency spectrum of ILMs which is sampled along the bright line in Fig.1. The spectral distribution of the moving ILMs is represented by an extended wavenumber-frequency domain since it does not end in the  $[0, 2\pi]$  range. For static ILMs, spectral distribution is symmetric at  $k = \pi$ . For moving ILMs, although the shape of the spectral distribution is similar to that of the static one, the center of the distribution is shifted to the lower wavenumber side. Figure 3 shows the deviation of the center from  $k = \pi$  for various moving ILMs with  $T_c$ . For the same  $T_c$ , there is a linear relationship between the moving velocity and the deviation from the center. Therefore, the deviation is easily obtained for any desired velocities.

Figure 4 shows a comparison of the wavenumber-frequency spectrum of the static ILM and the moving ILM with the same  $T_c$ . The spectrum for the moving ILM is shifted using the linear relationship shown in Fig.3. The blue curve is obtained by shifting the center of the spectrum to  $k = \pi$  and the red curve is obtained by folding the spectrum in adjacent Brillouin zones into the 1st Brillouin zone after the wavenumber shift. These are well matched and we can assume that the spectrum of static ILMs is folded into the 1st Brillouin zone.

In summary, the three things about differences in wavenumber-frequency spectra between the static and moving ILMs are important: the slope of the distribution, the shift of the center position, and the assumption that the spectrum of static ILMs is folded. In the next section, based on the above, we will explain how to estimate the initial conditions by reconstructing the wavenumber-frequency spectrum of the moving ILM from that of the

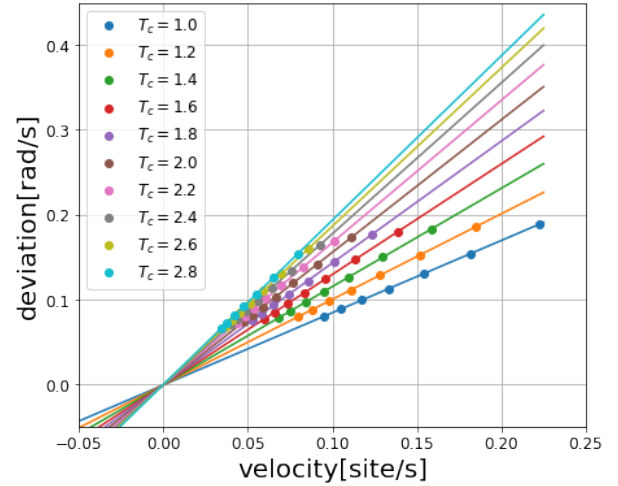


Figure 3: Relation between velocity and deviation

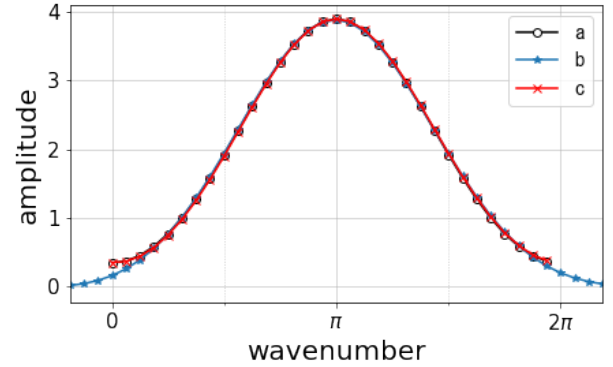


Figure 4: shifted and folded wavenumber-frequency spectrum (a: static ILM, b: shifted moving ILM, c: shifted and folded moving ILM)

static ILM.

### 3. How to estimate the initial value of moving ILMs

This section describes a method for estimating the initial conditions of moving ILMs. First, we calculate the waveform of static ILMs with an exact solution and perform a 2D Fourier transform on the waveform. As shown in Fig.1(a), the spectrum  $\psi(k)$  is extracted along the bright line appearing in the wavenumber-frequency domain. Next, the following function,

$$\begin{aligned} \psi(k) &= A \left( e^{-\frac{(k+\pi)^2}{2c^2}} + e^{-\frac{(k-\pi)^2}{2c^2}} + e^{-\frac{(k-3\pi)^2}{2c^2}} \right) + h(k) \quad (0 < k < 2\pi) \\ &= g(k) + h(k) \end{aligned} \quad (3)$$

is fitted to the extracted spectrum to determine  $A$  and  $c$  of Gaussian functions of  $g(k)$ . In Eq.(3),  $e^{-\frac{(k+\pi)^2}{2c^2}}$  represents the folded spectrum from  $[-2\pi, 0]$  and  $e^{-\frac{(k-3\pi)^2}{2c^2}}$  from

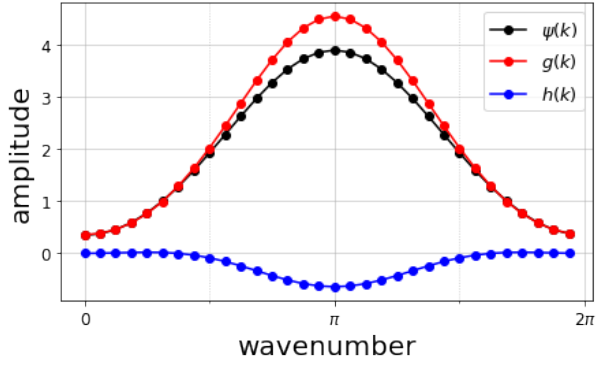


Figure 5: Division of Fourier spectrum of static ILMs

$[2\pi, 4\pi]$ . Figure 5 shows  $g(k)$  and  $h(k)$  in Eq.(3). The extracted spectrum is successfully decomposed to the folded Gaussian functions and a strongly localized component. To construct the spectrum of the moving ILM, we shift the center of distribution to the lower wavenumber side based on the relationship between the deviation of the center of spectrum and the desired velocity shown in Fig.3. Let the absolute value of the deviation from the center be  $\delta$ . The wavenumber-frequency spectrum  $\bar{\psi}(k)$  can be expressed as follows:

$$\bar{\psi}(k) = Ae^{-\frac{(k-\pi+\delta)^2}{2\sigma^2}} + h(k+\delta) \quad (-2\pi < k < 4\pi). \quad (4)$$

The obtained Fourier spectral distribution is placed in the frequency-wave number domain with a slope corresponding to the desired velocity. An initial condition is obtained by the inverse Fourier transformation. In practice, the initial position  $u_n(0)$  is obtained according to the following equation,

$$u_n(0) = \sum_{k=-2\pi}^{4\pi} \bar{\psi}(k)e^{-kn}. \quad (5)$$

Since  $d/dt$  becomes  $-i\omega$  in the wavenumber-frequency domain, the initial velocity can be obtained by multiplying  $-i(\omega_c - V_b(\pi - k))$  to Eq.(5) as follows:

$$v_n(0) = \sum_{k=-2\pi}^{4\pi} (-i(\omega_c - V_b(\pi - k))\bar{\psi}(k)e^{-kn}, \quad (6)$$

where  $V_b$ [site/s] is the velocity of the moving ILM. In this way, we can generate initial values for various velocities  $V_b$ . Since higher harmonics also appear in the wavenumber-frequency domain, the third and fifth harmonics are also taken into account in the calculations for accuracy.

#### 4. Result of estimation

Figure 6 shows an example of estimation results generated according to Sec.3. It can be seen that both the initial position and the velocity are localized. The numerical simulation started from the obtained initial conditions is shown

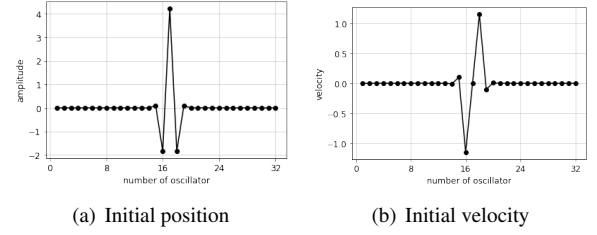


Figure 6: Result of estimation

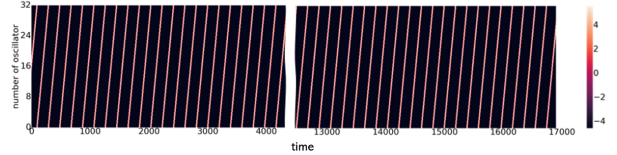


Figure 7: Energy transitionion

in Fig.7, which shows the time evolution of the energy of each oscillator. The energy  $e_n(t)$  of each oscillator is defined as follows:

$$\begin{aligned} e_n(t) = & \frac{1}{2}\dot{u}_n(t)^2 + \frac{\alpha_1}{2}u_n(t)^2 + \frac{\beta_1}{4}u_n(t)^4 \\ & + \frac{1}{2}\left(\frac{\alpha_2}{2}(u_n(t) - u_{n-1}(t))^2 + \frac{\beta_2}{4}(u_n(t) - u_{n-1}(t))^4\right) \\ & + \frac{1}{2}\left(\frac{\alpha_2}{2}(u_n(t) - u_{n+1}(t))^2 + \frac{\beta_2}{4}(u_n(t) - u_{n+1}(t))^4\right). \end{aligned} \quad (7)$$

The localization is maintained for a sufficiently long period. This implies that the estimated initial condition is sufficiently precise.

To investigate the efficacy of the estimation method, the lifetime of generated moving ILMs are measured for various  $T_c$  and  $V_b$ . To evaluate the lifetime, the center of the moving ILM is first computed[7] by

$$X = \frac{\arg h}{2\pi}N \quad (8)$$

where

$$\begin{aligned} h = & \sum_{n=1}^N \left\{ \left( \frac{1}{2}\dot{u}_n^2 + \frac{\alpha_1}{2}u_n^2 + \frac{\beta_1}{4}u_n^4 \right) e^{i\frac{2\pi}{N}n} \right. \\ & \left. + \left( \frac{\alpha_2}{2}(u_n - u_{n-1})^2 + \frac{\beta_2}{4}(u_n - u_{n-1})^4 \right) e^{i\frac{2\pi}{N}(n-\frac{1}{2})} \right\}. \end{aligned} \quad (9)$$

The energy of the core of the ILM is defined as follows:

$$E_{\text{core}}(t) = \sum_{n=m-4}^{m+4} e_n(t), \quad (10)$$

where  $m$  is the rounded integer of the center  $X$ . Then the ratio of the core energy at  $t$  to the initial core energy is defined as follows:

$$\gamma(t) = \frac{E_{\text{core}}(t)}{E_{\text{core}}(0)}. \quad (11)$$

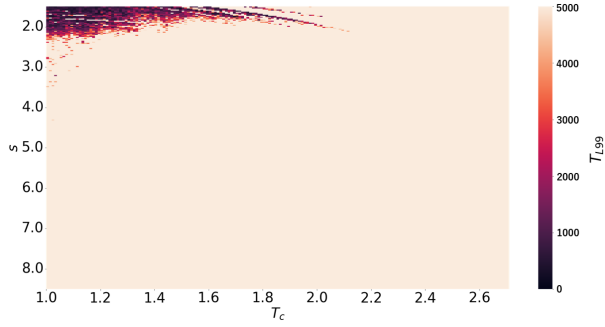


Figure 8:  $T_{L99}$  for various  $T_c$  and  $s$

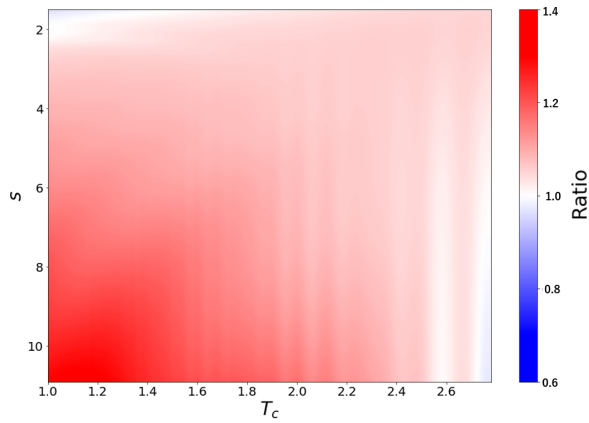


Figure 9: Ratio of the obtained and set velocity for various  $T_c$  and  $s$

The first time  $T_{L99}$  that satisfies  $\gamma(t) < 0.99$  is used as an indicator of the localization lifetime[5]. Figure 8 shows  $T_{L99}$  for various  $T_c$  and  $s = \frac{1}{T_c V_b}$ . The simulation length is limited to 5000[s]. The brightness corresponds to the lifetime of generated moving ILMs. The localization is generally maintained in a wide range and this method can be applied to various settings. In the high velocity and high energy region, there are cases where the lifetime becomes short, which will be investigated in future work.

Figure 9 shows the ratio of the obtained and desired moving velocity for various  $T_c$  and  $s$ . The velocity of generated moving ILM,  $V_b$ , is measured at the beginning of the simulation, and  $s$  is computed by  $s = 1/(T_c V_b)$ . We measured velocity immediately after starting the calculation. The estimated initial condition generates rather faster moving ILM than the desired one. The reason for it will be examined in future work.

## 5. Conclusion

In this report, we describe a method for estimating the initial conditions of moving ILM using a spectrum of static ILMs in the wavenumber-frequency domain. This method allows us to set a continuous value for the moving velocity, unlike the numerically exact solution. We will apply this

estimation method to other models in the future.

## References

- [1] A. J. Sievers and S. Takeno, “Intrinsic localized modes in anharmonic crystals”, *Phys. Rev. Lett.*, vol.61, pp.970-973, 1988.
- [2] S. Flach and A.V. Gorbach, “Discrete breathers – advances in theory and applications”, *Phys. Rep.*, vol.467, pp.1–116, 2008
- [3] M. Sato et al. “Experimental investigation of supertransmission for an intrinsic localized mode in a cyclic nonlinear transmission line”, *Chaos* 32, 033118, 2022
- [4] J. Bajars et al. “Nonlinear propagating localized modes in a 2D hexagonal crystal lattice”, *Physica D* vol.301-302, pp.8-20, 2015
- [5] M. Kimura and S. Doi, “A study on initial value estimation for moving intrinsic localized modes in ring coupled oscillator”, *Technical Report of IEICE*, vol. 116, no. 523, NLP2016-119, pp.69-74, 2017
- [6] M. Sato et al., “Supertransmission channel for an intrinsic localized mode in a one-dimensional nonlinear physical lattice”, *Chaos* 25 103122, 2015
- [7] M. Kimura et al. “Parametric resonance of intrinsic localized modes in coupled cantilever arrays”, *Physics Letters A*, vol.380, pp.2823-2827, 2016